Biomedicine & Pharmacotherapy 123 (2020) 109781

Contents lists available at ScienceDirect

Biomedicine & Pharmacotherapy

journal homepage: www.elsevier.com/locate/biopha

The stilbene and dibenzo[*b,f*]oxepine derivatives as anticancer compounds

Damian Garbicz[a], Piotr Tobiasz[b], Filip Borys[b], Tomasz Pilżys[a], Michał Marcinkowski[a], Marcin Poterała[b], Elżbieta Grzesiuk[a,*], Hanna Krawczyk[b,*]

[a] *The Institute of Biochemistry and Biophysics of the Polish Academy of Sciences, Pawinskiego 5a, 02-106 Warszawa, Poland*
[b] *Department of Organic Chemistry, Faculty of Chemistry, Warsaw University of Technology, Noakowskiego 3, 00-664 Warsaw, Poland*

ARTICLE INFO

Keywords:
Stilbene
Dibenzo[*b,f*]oxepine
Cancerous cell lines
Tubuline
Molecular docking

ABSTRACT

In the present study, the synthesis and cytotoxic effect of six stilbenes and three oxepine derivatives against two cancerous – HeLa and U87, and two normal – EUFA30 and HEK293 cell lines has been reported. The results of cytotoxic assay and flow cytometry analysis revealed that compounds 9-nitrobenzo[*b*]naphtho[*1,2-f*]oxepine (**4**), (*E*)-3,3′,4,4′,5,5′-hexamethoxystilbene (**6**) and 4-hydroxy-2′,4′-dinitrostilbene (**8**) were the most active and their interaction with tubulin (crystal structure from PDB) has been analyzed by computer molecular modeling. Molecular docking of these compounds on colchicine binding site of the tubulin indicates the interaction of (**4**), (**6**) and (**8**) with tubulin. The compound (**4**) could interact stronger with tubulin, relative to colchicine, however, with no selectivity of action against cancer and normal cells. Conversely, compounds (**6**) and (**8**) interact more weakly with tubulin, relative to colchicine but they act more selectively towards cancerous versus normal cell lines. Obtained results proved that the compounds that are the most active against cancerous cells operate through tubulin binding.

1. Introduction

Microtubules display various functions in living cells. They form a cytoskeleton, allow intracellular transport, mobility, and also build a mitotic spindle to provide flexibility to the cell that is necessary to divide. In all eukaryotic cells, two globular proteins – α- and β-tubulin each about 50 kDa are present. These two molecules form an αβ-tubulin heterodimer with two guanosine triphosphate (GTP) molecules. In certain conditions, these heterodimers attach one to another in a head-to-tail manner and form protein fiber called protofilament. Self-assembly of protofilaments results in the pipe-like structure, known as microtubule (Fig. 1).

In cells, microtubules are regulated mainly by their polymerization dynamics which is a reversible process with α- and β-tubulin heterodimers noncovalently added to both ends of microtubule [1]. The polymerization process is extremely fluid, with tubulin dimers added at one end, while dimers are removed from the other end. The transition between these two processes is known as dynamic instability. *In vitro,* tubulin polymerizes at a higher rate at the “plus end”, which ends with the β-subunit. The second end, called “minus end” is terminated with the α-subunit and polymerizes at slower motion [2].

The microtubule network presented during interphase is disassembled at the beginning of mitosis and replaced by a new network of spindle microtubules which are four to 100-fold more dynamic than the microtubule array in the interphase cytoskeleton [3]. If the microtubule dynamic is disrupted, the cell cycle is arrested in the mitosis phase on the interface between metaphase and anaphase leading to cell death. In the tubulin heterodimer structure, we can distinguish at least three characteristic drug binding sites that inhibit the microtubule activity. Those are: vinca alkaloids binding site (vinblastine binding site) located in the proximity of GTP binding site at β-tubulin subunit, paclitaxel binding site situated at interfilament region of β-tubulin and colchicine binding site first described in 2004 by Ravelli et al. located at the interface between α- and β-tubulin heterodimer [4]. Drugs applicable in clinical oncology occupied only the first two of these sites [5]. Microtubule targeting agents (MTA) depending on their structure, bound with a certain region of tubulin and can interfere with microtubule dynamics in two different manners. The first group consists of the microtubule-stabilizing agent. These include compounds that bind to the paclitaxel domain: taxanes, epothilones, and discodermolide. The second group – microtubule-destabilizing agents includes many vinca alkaloids and compounds that bind to the colchicine domain. Both microtubule-stabilizing and destabilizing agents influence the dynamics and stability of the microtubules even in low concentrations [6]. Impaired microtubule activity causes abnormalities in the functioning of cells functions. Due to the fact that cancer cells are characterized by

* Corresponding authors.
E-mail addresses: elag@ibb.waw.pl (E. Grzesiuk), hkraw@ch.pw.edu.pl (H. Krawczyk).

https://doi.org/10.1016/j.biopha.2019.109781
Received 29 August 2019; Received in revised form 27 November 2019; Accepted 4 December 2019

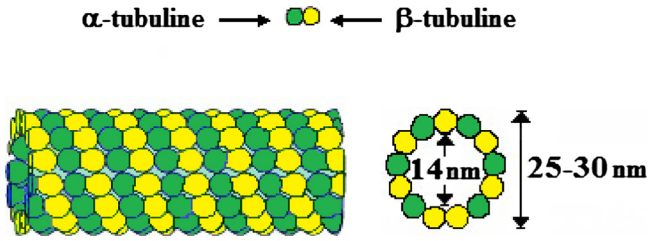

Fig. 1. Microtubule structure.

more frequent divisions in comparison to normal cells, they are also more sensitive to substances that interfere with this process [6]. Therefore, compounds that are inhibitors of microtubule activity are treated as potential drugs that may be effective in treating cancer. Over past decades, extensive studies towards compounds interacting with the colchicine binding site have been conducted [7–11]. However, no microtubule inhibitor has been found clinically applicable. Colchicine (Fig. 2) has been found as the first drug binding tubulin very tightly, nevertheless its use in the clinical cancer treatment has been hampered due to its severe toxicity to normal tissues [12].

Stilbenoids are naturally present in plants and make an important contribution to biochemical and physiological processes acting also as natural protective agents to defend the plant against viral and microbial attack, excessive UV exposure, and diseases. In human, they have been used as drugs and antitumor agents. Nowdays, combretastatins are perceived as the most promising microtubule targeting agents binding the colchicine binding site [13]. Combretastatins CA-1 and CA-4 belonging to naturally occurring stilbene derivatives are new vascular targeting and vascular disrupting agents (Fig. 2) [14]. They possess outstanding properties to inhibit gastric tumor metastasis and to increase antitumor immune reactivity [15]. CA-1P is the sodium diphosphate prodrug derived

from combretastatin A1, initially isolated form African plant *Combretum caffrum,* exhibiting remarkable antineoplastic and vascular-disrupting activities [16,17]. *In vivo*, combretastatin A1 diphosphate (CA-1P) is enzymatically dephosphorylated to the active form of combretastatin A1 (CA-1) which causes microtubule depolymerization, endothelial cell mitotic arrest, and apoptosis [18]. The disodium phosphate salt of CA-4 (Fosbretabulin) is under phase II/III of a clinical trial, additionally combined with other anticancer drugs [19]. It is also worth noticing that the other stilbene compounds have been shown to possess potent anticancer, anti-inflammatory, and antioxidant activities [20]. The high mortality of cancer patients results from too late or inadequate diagnosis of the disease itself and still inadequately effective therapy. Chemotherapy is one of the most common methods of treatment, however, despite the use of cytostatic, further growth of cancer cells is still observed. This is mainly due to the creation of multidrug resistance (MDR) mechanisms. Microtubule binding drugs lead, among others, to primary resistance being a result of the character of tissue the tumor originated. This is achieved by changes in the expression of the MDR repressive gene. The second type is acquired resistance, which arises in cells originally sensitive to chemotherapy. The most common cause of resistance is overexpression of the MDR1 gene encoding P-glycoprotein (Pgp), lowering the intracellular concentration of the drug and its cytotoxicity. That leads to arising the population of mutant cells with increased expression of Pgp, thus the drugs act only on the population of sensitive cells. P-glycoprotein is a member of a vast family of structurally similar proteins found in all groups of organisms from prokaryotes to *Homo sapiens*. This family is known as ABC carriers (ATP-binding cassette transporter) binding a broad range of compounds. Adenosine triphosphate (ATP) is also bounded to ABC carriers and energy form its hydrolysis is utilized for translocation of the bounded drug to extracellular space [21]. All compounds applicable in clinical oncology (e.g. vinblastine, taxol, vincristine) target vinca alkaloids or taxanes binding sites of tubulin. Despite their high potency, clinical usage is still limited mainly because of following reasons:

1) In many cases, there is a high probability of developing multi-drug resistance.
2) Their high lipophilicity enforces usage of surfactants (e.g. Tween 80). This may lead to hypersensitivity of some patients.
3) Due to low solubility in water their administration is restricted to intravenous injection.

These adverse effects can be largely overcome by the use of compounds that bind to the colchicine binding site, for example, many of them possess high solubility in water, and hence they can be administrated orally. Moreover, there is no need to use additives improving solubility, thus there is no risk of hypersensitive reactions. The most important, they do not lead to the incurred resistance to CA4P, thus not influencing its clinical efficacy [22]. In addition, beyond overexpression of ABC carriers, the causes of drug resistance are tubulin mutations, occuring after the use of paclitaxel or vinorelbine. Tubulin mutations and changes in the expression of individual isotypes can induce drug resistance, either directly by reducing the affinity of drugs to tubulin, or indirectly through changes in the dynamics of microtubules [23]. Drugs that bind the colchicine domain, e.g. colchicine or stilbenoids do not affect the expression of β-tubulin [24].

Continuing our study concerning the synthesis and search for biologically active stilbenes, [25–27] we have directed our attention also to the dibenzo[*b,f*]oxepines. These compounds have (Z)- stilbene motif in their skeletons, and additionally, their aromatic rings are connected by oxygen. Moreover, dibenzo[*b,f*]oxepine is an important scaffold in medicinal chemistry and its derivatives occur in several medicinally important plants [28–32]. We investigated also hydroxy and methoxy derivative of *E*-stilbenes, because there are known compounds e.g. resveratrol (RES, (*E*)-3,5,4′-trihydroksystilben) having medical effects. Resveratrol is a polyphenol produced by plant species and has been widely studied due to its ability to inhibit the growth of cancer cells [33]. Another active stilbene is pterostilbene (4-[(*E*)-2-(3,5-dimethoxyphenyl)ethenyl]phenol) which exhibits lipid and glucose-lowering effects used in the treatment of resistant hematology malignancies. I also has antioxidant capacity and demonstrates concentration-dependent anticancer activity [34–37]. There are only few data regarding their activity as microtubule targeting agents [38].

2. Material and methods

2.1. Chemistry

Substrate (**2**) are commercially available from Sigma-Aldrich and

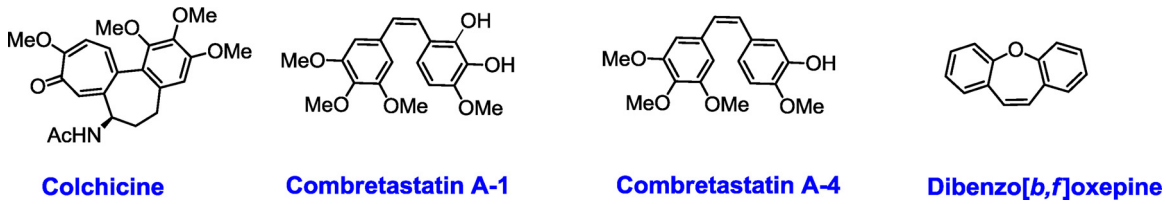

Fig. 2. Structure of colchicine, of combretastatin A-1, of combretastatin A-4 and of dibenzo [*b,f*]oxepine.

was protected with an ethyl group according to [39], compounds (**1**) and (**3**) were synthesized according to literature procedures [26] and [27] respectively. Molecule (**6**) was prepared according to modified literature procedures: [27,33].

2.1.1. Synthesis of (5a) and (6)

To a well-stirred and cooled to 0 °C suspension of zinc powder (9.40 g, 143.8 mmol) in anhydrous THF (100.0 mL), titanium tetrachloride (13.62 g, 7.86 mL, 71.8 mmol) was added dropwise. The mixture was stirred at 0 °C for 0.5 h and then *p*-methoxybenzaldehyde (59.8 mmol) or solution of 3,4,5-trimethoxybenzaldehyde (59.8 mmol) in THF (25 ml) was slowly added. The suspension was refluxed for 24 h under argon, then cooled to 0 °C and diluted with cold water (200 mL). Zinc dust and precipitated stilbene were filtered off, washed with distilled water (2 × 50 mL) and methanol (2 × 25 mL) and dried under vacuume. After recrystallization and hot filtration, pure stilbene was obtained.

(*E*)-4,4′-dimethoxystilbene (**5a**), Yield 68 %, product was crystallized from toluene/ethyl acetate. ^{1}H NMR ($CDCl_3$, 500 MHz): δ 3.83 (s, 6H, CH_3O), 6.88–6.91 (m, 4H, Ar), 6.93 (s, 2H, CH = CH), 7.41–7.44 (m, 4H, Ar). ^{13}C NMR ($CDCl_3$, 125 MHz): δ 55.5, 114.3, 126.3, 127.6, 130.6, 159.2. FTIR (ν_{max}/ cm^{-1}): 3069, 3017, 2955, 2937, 2911, 2838, 2051, 1987, 1894, 1832, 1606, 1575, 1511, 1464, 1447, 1440, 1425, 1306, 1269, 1244, 1214, 1177, 1152, 1110, 1027, 967, 955, 832, 824, 815, 744, 728, 640. HRMS (ESI): $C_{16}H_{16}O_2Na+$, calcd *m/z* 263.1048 ; found *m/z* 263.1049.

(*E*)-3,3′,4,4′,5,5′-hexamethoxystilbene (**6**), Yield 81 %, product was crystallized from toluene. ^{1}H NMR ($CDCl_3$, 500 MHz): δ 3.87 (s, 6H, CH_3O), 3.91 (s, 12H, CH_3O), 6.73 (s, 4H, Ar), 6.93 (s, 2H, CH = CH). ^{13}C NMR ($CDCl_3$, 125 MHz): δ 56.2, 61.1, 103.6, 128.2, 133.0, 138.0, 153.5. FTIR (ν_{max}/ cm^{-1}): 3006, 2976, 2941, 2833, 1583, 1508, 1464, 1418, 1350, 1316, 1263, 1248, 1231, 1187, 1119, 993, 966, 919, 830, 782, 675, 651. HRMS (ESI): $C_{20}H_{24}O_6Na+$, calcd *m/z* 383.1471; found *m/z* 383.1470.

2.1.2. Synthesis of (5)

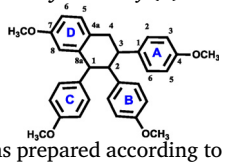

was prepared according to literature procedures [27]: 7-methoxy-1,2,3-tris(4-methoxyphenyl)-1,2,3,4-tetrahydronaphthalene (**5**). White solid, yield: 432 mg (90 %), m.p. 139−140 °C (EtOH). ^{1}H NMR (500 MHz, $CDCl_3$, 298 K): δ (ppm): **the ring**: 3.06 (1H, AB spin system, dd ^2J = -16.5 Hz, ^3J = 4.5 Hz, H4), 3.18 (1H, AB spin system, dd, ^3J = 11.5 Hz, H4′), 4.18 (1H, d, ^3J = 10.5 Hz, H1), 3.15 (1H, dd, ^3J = 11 Hz, H2), 3.33 (1H, ddd, H3); **A ring**: 6.75 (2H, d, ^3J = 8.5 Hz, H2,H6), 6.66 (2H, d, H3,H5), 3.74 (3H, s, OCH_3); **B ring** 6.68 (2H, d, ^3J = 8.5 Hz, H2, H6), 6.52 (2H, d, H3, H5), 3.65 (3H, s, OCH_3); **C ring**: 6.98 (2H, d, ^3J = 8.5 Hz, 1 H2, H6), 6.64 (2H, d, H3, H5), 3.70 (3H, s, OCH_3); **D ring** 7.07(1H, d, ^3J = 8.5 Hz, H5), 6.34 (1H, d, ^4J = 2.5 Hz, H8), 6.72 (1H, dd, H6), 3.63 (3H, s, OCH_3). ^{13}C NMR (125 MHz, CDCl3, 298 K): δ (ppm): **the ring**: 55.02(C1), 55.53(C2), 46.35(C3), 39.65(C4); **A ring**: 137.58(C1), 130.19(C2,C6), 113.45(C3,C5), 157.64 (C4), 55.09(OCH_3); **B ring**: 135.18(C1), 129.26(C2,C6), 113.03 (C3,C5), 157.18(C4) 54.91 (OCH_3); **C ring**: 136.82(C1), 128.52 (C2,C6), 113.33 (C3,C5), 157.45(C4),55.06 (OCH_3); **D ring** 129.37 (C4a), 129.06 (C5), 112.07 (C6), 157.75 (C7), 114.86 (C8), 141.45 (C8a), 55.20(OCH_3). HRMS (ESI): $C_{32}H_{32}O_4Na+$, calcd *m/z* 503.2198; found *m/z* 503.2195.

2.1.3. Synthesis of (4, 10)

A mixture of aromatic aldehyde (12 mmol) and 2.19 g (12 mmol) of 2,4-dinitrotoluene was ground in a mortar and then placed in a thick-walled glass test tube with a Teflon closure and 1.09 mL (0.937 g, 11.0 mmol) of piperidine was added. The contents of the vessel were heated at 90 °C for 2 h under argon, then dissolved in 150 mL of ethyl acetate and washed with 0.25 M hydrochloric acid (2 × 25 mL) and water to neutral pH. Then, the solvent and the remaining water were removed in vacuo and the crude product was purified by crystallization from methanol or ethanol with the additive of charcoal. After hot filtration, a pure stilbene was obtained.

9-nitrobenzo[*b*]naphtho[*1,2-f*]oxepine (**4**), Yield 29 %, product was crystallized from methanol, ^{1}H NMR (500 MHz, $CDCl_3$): δ 7.04 (d, 1H, J = 11.5 Hz, CH=), 7.35 (d, 1H, J = 8.5 Hz, Ph-NO_2), 7.42 (d, 1H, J = 9.0 Hz, Napht), 7.48 (ddd, 1H, J = 8.0, J = 7.0, J = 1.5 Hz, Napht), 7.57 (ddd, 1H, J = 8.0, J = 7.0,J = 1.5 Hz, Napht), 7.64 (d, 1H, J = 11.5 Hz, CH=), 7.83–7.85 (m, 1 H), 7.886 (d, 1H, J = 9.0 Hz, Napht), 8.00 (dd, 1H, J = 2.5 Hz, J = 8.5 Hz, Ar-NO_2), 8.05 (dd, 1H, J = 8.5 Hz, J = 1.0 Hz), 8.08 (d, 1H, J = 2.5 Hz, Ar-NO_2). ^{13}C NMR (125 MHz, $CDCl_3$): δ 117.0, 120.3, 121.1, 123.3, 123.4, 125.7, 127.5, 128.8, 129.2, 129.3, 130.1, 131.5, 131.6, 131.9, 137.9, 148.7, 156.0, 157.7. FTIR (ν_{max}/cm-1) 3101, 3074, 3037, 1615, 1591, 1522, 1483, 1438, 1400, 1341, 1320, 1227, 1207, 1191, 1149, 1129, 1078, 1062, 925, 896, 858, 850, 821, 808, 794, 760, 737, 725, 690, 670, 635. HRMS (ESI): $C_{18}H_{11}NO_3Na+$,calcd. *m/z* 312.0637- found 312.0638.

3-ethoxy-4-hydroxy-2′4′-dinitrostilbene (**10**) Yield 41 %, the product was crystallized from ethanol. ^{1}H NMR (500 MHz, $CDCl_3$): δ 1.50 (t, 3H, J = 7.0 Hz, CH_3), 4.19 (q, 2H, J = 7.0 Hz, CH_2O), 5.92 (s, 1H, OH), 6.95 (d, 1H, J = 8.0 Hz, Ar-3-CH_3CH_2O-4-OH), 7.07–7.09 (m, 2H, Ar-3-CH_3CH_2O-4-OH), 7.23 (d, 1H, J = 16.0 Hz, CH=), 7.45 (d, 1H, J = 16.0 Hz, CH=), 7.95 (d, 1H, J = 9.0 Hz, Ar-2,4-NO_2), 8.38 (ddd, 1H, J = 0.5 Hz, J = 2.5, J = 9.0 Hz, Ar-2,4-NO_2), 8.78 (d, 1H, J = 2.5 Hz, Ar-2,4-NO_2). ^{13}C NMR (125 MHz, $CDCl_3$): δ 14.9, 64.9, 109.7, 114.9, 118.6, 120.9, 122.8, 127.1, 128.3, 128.5, 138.5, 139.2, 145.9, 146.4, 147.3, 147.9. FTIR (νmax/cm-1) 3493, 3116, 2988, 2944, 2887, 1625, 1601, 1586, 1555, 1513, 1474, 1443, 1432, 1401, 1381, 1342, 1327, 1303, 1291, 1275, 1261, 1238, 1218, 1194, 1170, 1141, 1126, 1061, 1043, 973, 967, 962, 937, 920, 904, 852, 834, 826, 813, 737, 727, 713, 682. HRMS (ESI) : $C_{16}H_{14}N_2O_6Na+$, calcd. *m/z* 353.0749 -found 353.0748.

2.1.4. Synthesis of (7, 8, 9)

To a stirred mixture of 2,4-dinitrotoluene (2.19 g, 12 mmol), aldehyde (12 mmol) and toluene (20 ml) under argon, dry piperidine (1.09 ml, 0.937 g, 11.0 mmol) was added. After 3 h of heating at 90 °C, the solvent was distilled off on a rotary evaporator. Then ethyl acetate (150 mL) was added to the residue, and the resulting mixture was washed with 0.5 M hydrochloric acid (2 × 40 mL) and water to neutral pH. Next, the solvent and the remaining water were removed in vacuo and the crude product was purified by crystallization from methanol or ethanol with the additive of charcoal. After hot filtration, pure stilbene was obtained.

3-hydroxy-2′,4′-dinitrostilbene (**7**), Yield 22 %, product was crystallized from ethanol, ^{1}H NMR (500 MHz, DMSO-D_6, 30 °C): δ 6.80 (ddd, 1H, J = 8.0 Hz, J = 2.5 Hz, J = 1.0 Hz, Ar-3-OH), 7.05–7.09 (m, 2H, Ar-3-OH), 7.24 (t, 1H, J = 8.0 Hz, Ar-3-OH), 7.43 (d, 1H, J = 16.5 Hz, CH=), 7.51 (d, 1H, J = 16.5 Hz, CH=), 8.26 (d, 1H, J = 8.5 Hz, Ar-2,4-NO_2), 8.48 (ddd, 1H, J = 8.5 Hz, J = 2.5 Hz, J = 0.5 Hz, Ar-2,4-NO_2), 8.74 (d, 1H, J = 2.5 Hz, Ar-2,4-NO_2), 9.56 (s, 1H, OH). ^{13}C NMR (125 MHz, DMSO-D_6, 30 °C): δ 113.6, 116.7, 118.7, 120.2, 120.9, 127.1, 129.2, 129.9, 136.9, 137.5, 137.6, 145.8, 147.2, 157.7. FTIR (νmax/cm-1): 3429, 3094, 2356, 1627, 1594, 1580, 1515, 1344, 1290, 1254, 1211, 1168, 1153, 1125, 1091, 1064, 997, 978, 950, 922, 905, 876, 849, 833, 770, 755, 741, 727, 700, 678, 654, 605, 580. HRMS (ESI): $C_{14}H_{10}N_2O_5Na+$, calcd. *m/z* 309.0487- found 309.0489.

4-hydroxy-2′,4′-dinitrostilbene (**8**), Yield 14 %, the product was crystallized from a small amount of methanol. ^{1}H NMR (500 MHz, DMSO-D_6): δ 6.83 (d, 2H, J = 9.0 Hz, Ar-4-OH), 7.27 (d, 1H, J = 16.0 Hz, CH=), 7.50–7.55 (m, 3H, Ar-4-OH and CH=), 8.21 (d, 1H, J = 9.0 Hz, Ar-2,4-NO_2), 8.43 (dd, 1H, J = 9.0 Hz, J = 2.5 Hz, Ar-2,4-NO_2), 8.70 (d, 1H, J = 2.5 Hz, Ar-2,4-NO_2), 9.94 (s, 1H, OH). ^{13}C

NMR (125 MHz, DMSO-D_6): δ 115.9, 117.2, 120.4, 126.9, 127.0, 128.5, 129.4, 137.9, 138.1, 145.1, 146.8, 159.1. FTIR (νmax/cm-1): 3462, 3097, 3071, 1624, 1612, 1591, 1578, 1513, 1339, 1320, 1278, 1267, 1235, 1209, 1196, 1173, 1148, 1128, 1109, 1064, 975, 962, 941, 914, 874, 860, 836, 831, 822, 792, 760, 739, 728, 713, 685, 651, 641. HRMS (ESI): $C_{14}H_{10}N_2O_5Na+$, calcd. *m/z* 309.0487- found 309.0486.

3-hydroxy-4-methoxy-2′,4′-dinitrostilbene (**9**), Yield 60 %, product was crystallized from ethanol. ^{1}H NMR (500 MHz, $CDCl_3$): δ 3.81 (s, 3H, CH_3O), 6.98 (d, 1H, J = 8.5 Hz, Ar-3-OH-4-OCH_3), 7.08 (dd, 1H, J = 8.5 Hz, J = 2.0 Hz, Ar-3-OH-4-OCH_3), 7.12 (d, 1H, J = 2.0 Hz, Ar-3-OH-4-OCH_3), 7.27 (d, 1H, J = 16.0 Hz, CH=), 7.51 (d, 1H, J = 16.0 Hz, CH=), 8.24 (d, 1H, J = 9.0 Hz, Ar-2,4-NO_2), 8.44 (ddd, 1H, J = 9.0 Hz, J = 2.5 Hz, J = 0.5 Hz, Ar-2,4-NO_2), 8.71 (d, 1H, J = 2.5 Hz, Ar-2,4-NO_2), 9.23 (s, 1 H). ^{13}C NMR (125 MHz, $CDCl_3$): δ 55.6, 112.1, 113.3, 118.1, 120.4, 120.5, 127.0, 128.6, 128.7, 137.8, 137.9, 145.3, 146.8, 146.9, 149.4. FTIR (νmax/cm-1): 3471, 3093, 3019, 2992, 2946, 2851, 1625, 1616, 1595, 1577, 1522, 1509, 1495, 1455, 1438, 1339, 1323, 1299, 1287, 1275, 1260, 1222, 1207, 1182, 1159, 1147, 1134, 1123, 1063, 1022, 967, 923, 901, 876, 864, 841, 834, 828, 811, 759, 737, 728, 719, 677, 651. HRMS (ESI): $C_{15}H_{12}N_2O_6Na+$, calcd. *m/z* 339.0593 -found 339.0594.

2.2. NMR measurements

All the spectra were recorded using a Varian VNMRS spectrometer operating at 11.7 T magnetic field. Measurements were performed for ca. 1.0 M solutions of all the compounds in DMSO-d_6 or $CDCl_3$. The residual signals of DMSO-d6 (2.54 ppm) and of $CDCl_3$ (7.26 ppm) in ^{1}H NMR and of the DMSO-d_6 signal (40.4 ppm) and of $CDCl_3$ (77.0 ppm) in ^{13}C NMR spectra were used as the chemical shift references. Spin multiplicities are described as s (singlet), d(doublet), t (triplet), q (quartet), m (multiplet), dd (double doublet). Coupling constants are reported in Hertz. All the proton spectra were recorded using the standard spectrometer software and parameters set: acquisition time 3 s, pulse angle 30°. The standard measurement parameter set for ^{13}C NMR spectra was: pulse width 7 μs (the 90° pulse width was 12.5 μs), acquisition time 1 s, spectral width 200 ppm, 1000 scans of 32 K data point were accumulated and after zero-filling to 64 K; and the FID signals were subjected to Fourier transformation after applying a 1 Hz line broadening. The ^{1}H-^{13}Cgs-HSQC and ^{1}H-^{13}Cgs-HMBC spectra were also recorded using the standard Varian software.

2.3. Biological evaluation

2.3.1. Cell culturing

HeLa, U87, HEK293, Eufa cell lines were cultured in DMEM medium (Life Technology) supplemented with 10 % fetal bovine serum (Life Technology) and 0.1 % antibiotics (penicillin, streptomycin, Life Technology). Cells were grown in a humidified atmosphere of CO_2/air (5/95 %) at 37 °C.

2.3.2. Cytotoxicity assay

Exponentially growing cells were seeded onto a 96-well plate at the density of 2 × 103 cells/well, cultured for 18 h, and treated with new derivatives at indicated concentrations (1–200 μM), or with DMSO as a control, for 24 or 48 h. Alamar Blue (Invitrogen) was added accordingly to the manufacturer protocol. After 4 h, light emission at 590 nm was measured with excitation at 560 nm using a scanning multiwell spectrophotometer (DTX 880, Beckman Coulter). The experiment was carried out at least three times with three replicates for each inhibitor concentration. After background subtraction, inhibition rates (IC50) were calculated as the concentration of the component inhibiting cell growth by 50 %. All the calculations were performed using Origin 9.0 software.

2.3.3. Flow cytometry

The Annexin V-FITC apoptosis detection kit (BD Biosciences) was used to detect apoptosis by flow cytometry. Cells were seeded at 6-well plates at a concentration of 5 × 105 cells/well, cultured for 18 h, and tested agent was applied for indicated periods. Subsequently, cells were washed with PBS, resuspended in binding buffer at a concentration of 2 × 106 cells/ml, and anti-Annexin V FITC-conjugated antibody and propidium iodide were added to 100 μl aliquots. The mixtures were incubated for 15 min at room temperature, supplemented with a binding buffer to 500 μl and processed by BD FACSCalibur (BD Biosciences). Data were analyzed in Flowing Software version 2.5.1 (Flowing Software, http://www.uskonaskel.fi/flowingsoftware).

2.4. Computational aspects

The optimum ground-state geometry for compounds (**4**), (**6**) and (**8**) was calculated using density functional theory (DFT) [40,41]. The B3LYP functional and 6-311++g (2d,p) basis set and the continuum model (PCM; Gaussian 03 W) [35,36]was used in order to simulate the effects of the solvent -DMSO. All calculations were performed on a server equipped with a 16 quad-core XEON (R) CPU E7310 processor operating at 1.60 GHz. The operating system was Open SUSE 10.3 (see Supplementary data).

2.4.1. Molecular docking simulations

The experimental crystal structure of tubulin (PDB entry: 1SA0) was used in docking experiments [42,43]. Chains A, B, E as well as GTP, GDP, magnesium ion and ligand were removed before docking from receptor structure. CYS241, LEU248, LYS254, LEU255, VAL315, ASN350, LYS352 and ILE378 were set as flexible residues. The Graphical User Interface (GUI), including python scripts for ligand and receptor preparation, was part of AutoDock Tools 1.5.6. AutoDock suite and AutoDocktools (ADT) are provided by the Scripps Research Institute (http://autodock.scripps.edu/). The optimum ground-state geometry of ligand compounds was calculated using the density functional theory (DFT). In calculation, the B3LYP functional and 6-311++g (2d,p) basis set was employed and the continuum model (PCM; Gaussian 03 W) [35,36] was used in order to simulate the effects of the solvent. The colchicine docking site was determined from the DAMA-colchicine crystallized structure. The centres of the box were set (X = 39.82, Y = 53.24, Z = -8.21) and its dimensions were set to 21 × 21 × 21 Å. The exhaustiveness parameter was equal to 8. Docking calculations were performed using AutoDock Vina software [44]. The best-docked structure was chosen using the binding energy score given by AutoDock Vina. All computations were performed on an Intel® CoreTM i7-4702MQ 3.2 GHz processor running Ubuntu 18.04 Workstation Linux distribution. PyMOL software (www.pymol.org/) was used to analyze the docking results [45]. The Protein-Ligand Interaction Profiler (PLIP) was used in order to predict protein-docked ligand interactions [46].

3. Results and discussion

Here we report the synthesis and cytotoxic effect of six stilbenes and three oxepine derivatives against two cancerous – HeLa and U87, and two normal – EUFA30 and HEK293 cell lines. We also performed molecular docking of these derivatives to tubulin (Fig. 3).

3.1. Chemistry

The routes synthetic are summarized in Scheme 1. Compounds (**1**), (**4**), (**7**)-(**10**) were obtained in two synthetic steps starting from the condensation of suitable aldehyde and 2,4-dinitrotoluene (Experimental section and Supplementary material). For dibenzo[*b,f*]oxepines the next step was the reaction between a derivative of 2,4-dinitrostilbene and sodium azide. In the reactions arise corresponding nitro-

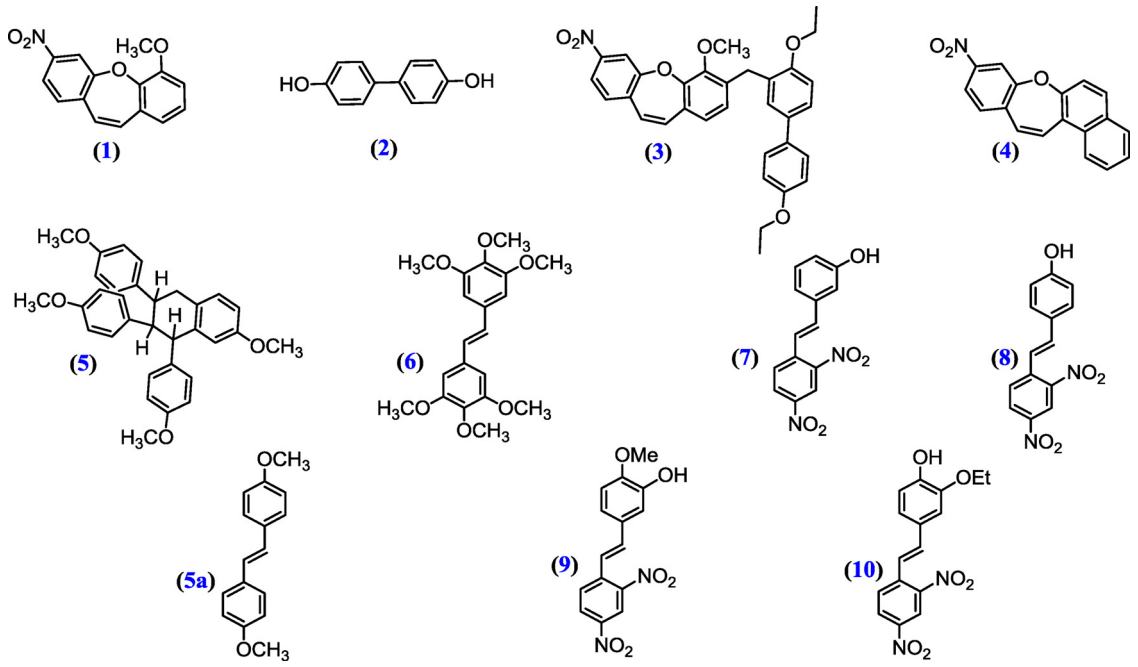

Fig. 3. The structure of: 6-methoxy-3-nitrodibenzo[*b,f*]oxepine (**1**), [1,1′-biphenyl]-4,4′-diol (**2**), 3-((4,4′-diethoxy-[1,1′-biphenyl]-3-yl)methyl)-4-methoxy-7-nitrodibenzo[*b,f*]oxepine (**3**), 9-nitrobenzo[*b*]naphtho[*1,2-f*]oxepine (**4**), 7-methoxy-1,2,3-tris(4-methoxyphenyl)-1,2,3,4-tetrahydronaphthalene (**5**), (*E*)-4,4′-dimethoxystilbene (**5a**), (*E*)-3,3′,4,4′,5,5′-hexamethoxystilbene (**6**), 3-hydroxy-2′,4′-dinitrostilbene (**7**), 4-hydroxy-2′,4′-dinitrostilbene (**8**), 3-hydroxy-4-methoxy-2′,4′-dinitrostilbene (**9**) and 3-ethoxy-4-hydroxy-2′4′-dinitrostilbene (**10**).

dibenzo[*b,f*]oxepine (**1**) and (**4**). The product (**1**) was a substrate in the reaction with paraformaldehyde in the presence of a Lewis acid as the catalyst ($BF_3{\cdot}OEt_2$) and with 4,4′-diethoxy-1,1′-biphenyl. This process was successfully conducted, which enables the incorporation of aryl groups, (product **3**) to the dibenzo[*b,f*]oxepin framework [27]. Stilbenes (**5a**) and (**5**) (**6**) was prepared according to modified literature procedures [47,27]: titanium tetrachloride and suitable methoxy aldehyde. In the reaction of stilbene (**5a**) with Lewis $BF_3{\cdot}OEt_2$ acid (the catalyst of cyclization reaction), it was obtained cyclic stilbene - tetralin (**5**) [25]. Compound (**5a**) and the ethyl ester of (**2**) were not tested because they did not dissolve in DMSO.

3.2. Cytotoxic effect of stilbenes and oxepines towards cultured normal and cancer cells

In the present study, we evaluated the cytotoxic efficacy of six stilbenes and three oxepine derivatives on two cancerous – HeLa and U87, and two normal – EUFA30 and HEK293 cell lines (concentrations tested: 1–300 μM, Fig. 4, Table 1). Stilbene/oxepin-mediated growth inhibition proceeded in a dose-dependent manner and the effect was stronger for HeLa than U87 cells and for Eufa than HEK293 cells. Generally, stilbenes were more cytotoxic than oxepins, and most of them were more toxic to cancerous than normal cells. Compounds with the smallest IC_{50} value and the highest selectivity were three stilbene - (**6**), (**8**), and (**9**), IC_{50} value for HeLa cells were 109.2, 35.6 and 112.9 μM comparing to 756.4, 162.2 and 504.4 μM for Eufa30 cells, respectively. Oxepine (**4**) was the compound with the best biological activity, but with no selectivity. Further tests were performed on stilbenes (**6**) and (**8**), and oxepine (**4**).

To measure apoptosis induction, cells were treated with 100 μM for 24 and 48 h with 100 μM of (**6**), of (**8**) and of (**4**) (Fig. 5). The experiment was performed on one normal (Eufa30), and one cancer (HeLa) cell lines. The HeLa cells were more sensitive to stilbenes (**6**) and (**8**), than Eufa30 cells. In Eufa30 cells, after 24 h of (**6**) treatment, no significant increase in apoptosis or/and necrosis was observed, whereas HeLa cells showed a significant increase in necrotic cells, namely, from 17.2 % in untreated to 61.5 % in treated cells. After treatment with (**8**), Eufa30 cells showed a significant increase in early apoptosis from 0.4% to 9.6% after 24 h, and from 0.7% to 18.2 % after 48 h of treatment. In HeLa cells, a significant increase in necrotic cells after 24 and 48 h of treatment from 17.2% to 31.4 % and from 20.2% to 64.6%, respectively, was observed. Interestingly, stilbenes (**6**) and (**8** showed different mechanism of action on normal and cancer cells – after stilbene treatment most of the Eufa30 cells were in the early stages of apoptosis, and HeLa cells in the necrosis phase. Oxepine (**4**) showed the strongest cytotoxic effect, however, with no selectivity of action against cancer and normal cells: about 90 % of the Eufa and Hela cells were observed to be in the late stage of apoptosis.

3.3. NMR spectra and computational analysis

In order to determine the structure of the reaction products oxepine (**1**,**3**,**4**) and stilbene derivatives (**5-10**) in solution, ^1H and ^{13}C NMR spectra of all of the products have been measured (Supporting information). The ^1H and ^{13}C NMR resonances were assigned unequivocally, based on the combined information from 1D and 2D NMR (gCOSY, gHSQC, and gHMBC) experiments. Coupling constants (^1H-^1H) were measured directly from resolution-enhanced 1D spectra and confirmed, when necessary, by homo-decoupling. gHSQC and gHMBC analysis allowed the assignment of the regiochemistry of the products. The optimum structures of the best biological activity compounds (**4**), (**6**) and (**8**) were calculated using the DFT B3LYP/6-311 + + G(2d, p) method (and with polarizable continuum model-PCM, Gaussian 03 W) [35,36] (see supporting information). Optimized geometry of compounds (**4**), (**6**) and (**8**) were used in molecular docking.

3.4. Molecular docking simulations to tubulin in colchicine binding site

The integration of computational and experimental investigations has been of great value in the identification and development of novel promising compounds. Broadly used molecular docking methods explore the ligand conformations adopted within the binding sites of

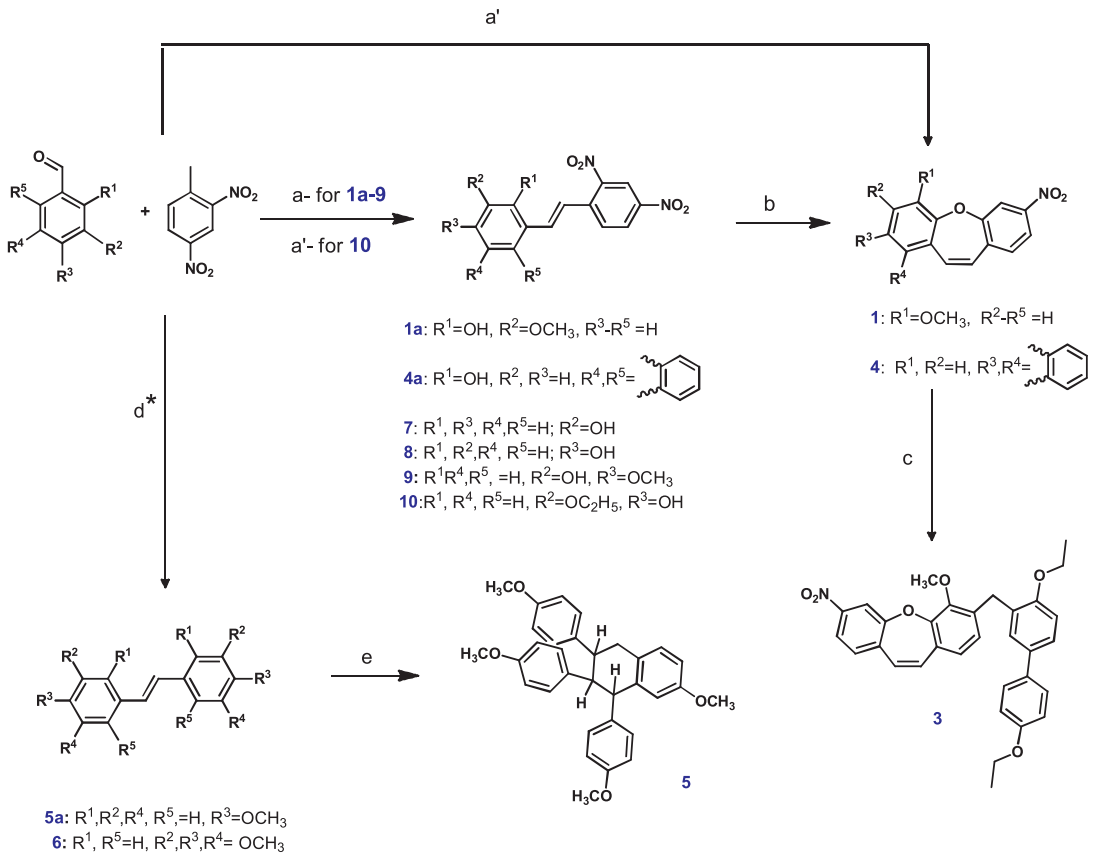

a)- piperidine, Ar,toluene, 90°C; a')-piperidine, Ar, 90°C; b)-NaN_3, DMSO,120°C, 24h; c)- 4,4'-diethoxy-1,1'-biphenyl, H_2CO,$BF_3O(C_2H_5)_2$, CH_2Cl_2, Ar, 25°C,3h; d*)- reaction only with respectively aldehyde without 2,4-dinitrotoluene, Zn,$TiCl_4$, THF, Ar and reflux 24h; e) -$BF_3O(C_2H_5)_2$,THF, Ar, 25°C, 3h

Scheme 1. Synthesis of dibenzo[*b,f*]oxepine (**1, 3, 4**) and stilbene derivatives (**1a**, **4a**, **5a**, **5**, **6**, **7**, **8**, **9**, **10**).

macromolecular targets. This approach also estimates the ligand-receptor binding free energy by evaluating critical phenomena involved in the intermolecular recognition process. Therefore, in our tests, the best active compounds (**4**), (**6**) and (**8**) to interact with tubulin (crystal structure from PDB code: 1SA0) [38] has been analyzed by computer molecular modeling. The molecular docking was performed by simulation of compound compounds (**4**), (**6**) and (**8**) into the colchicine binding site in tubulin (see supporting information). All docking runs were applied using the Broyden- Fletcher-Goldfarb-Shanno (BFGS) method of AutoDock Vina program [39]. The binding model of compounds (**4**), (**6**) (**8**) and tubulin is depicted in Fig. 6.

In the binding mode, compounds (**4**), (**6**), (**8**) bind to the colchicine binding site of tubulin via hydrophobic interactions and binding is stabilized by a hydrogen bond. The hydroxyl group of (**8**) behaves as a hydrogen bond acceptor, interacting with Lysβ254. The calculated binding energies were used as parameters for the selection of the cluster of docking posed to be evaluated (Fig. 6 a, b, c), in which the binding mode of the lowest energy structure was located (selection of the cluster in docking for the lowest energy structure of investigated molecule). The selected structure of (**4**), (**6**), (**8**) had an estimated binding free energy of -10.4, -7.0, -8.8 kcal/ mol respectively (binding free energy of control compounds colchicine and CA-4 are -8.6 kcal/mol and -7.62 kcal/mol, respectively [48]). The model was similar to the models between colchicine, CA-4 and the colchicine binding site [49,50]. In the (**4**) binding model, more details revealed that there were some key roles of the interaction between (**4**) and tubulin (Fig. 6a). The compound (**4**) was embedded in the hydrophobic pocket occupied by the A ring of colchicine (van der Waals contact with Alaβ316, Lysβ254, Alaβ250, and Leuβ248). The next compound (**6**) also interact with Leuβ248 and Leuβ255. The product (**8**) affects Leuβ248 and Lysβ254. These results suggest that compound (**4**) could interact stronger and compounds (**6**) and (**8**) less with tubulin, relative to colchicine and CA-4.

4. Conclusion

In summary, we have developed an easy and high-yielding synthesis for compounds **5**, **5a**, **6, 8** and **9** (which are the derivatives of dibenzo [*b,f*]oxepine or stilbene) from respectively substituted benzaldehydes and 2,4-dinitrotoluene. Molecules **4**, **7**, **8** and **10** were obtained with lower yields. The cytotoxic effect of all obtained products to two cancerous (HeLa and U87), and two normal (EUFA30 and HEK293) cell lines were measured. Notably, the most active compounds were one dibenzo[*b,f*]oxepine (**4**) and two stilbene derivatives, (**6**) and (**8**). Analysis of the binding model of the most active compounds (**4**), (**6**) and (**8**) with tubulin allowed to discover several interactions with the protein residues in the colchicine binding site. The compound (**4**) could interact stronger with tubulin, relative to colchicine, however, with no selectivity of action against cancer and normal cells. Inversely, compounds (**6**) and (**8**) interact weaker with tubulin, relative to colchicine but they act more selectively towards cancerous versus normal cell lines. Presented results are valuable premise to look for more powerful anticancer drugs based on the mechanism of inhibition of tubulin polymerization.

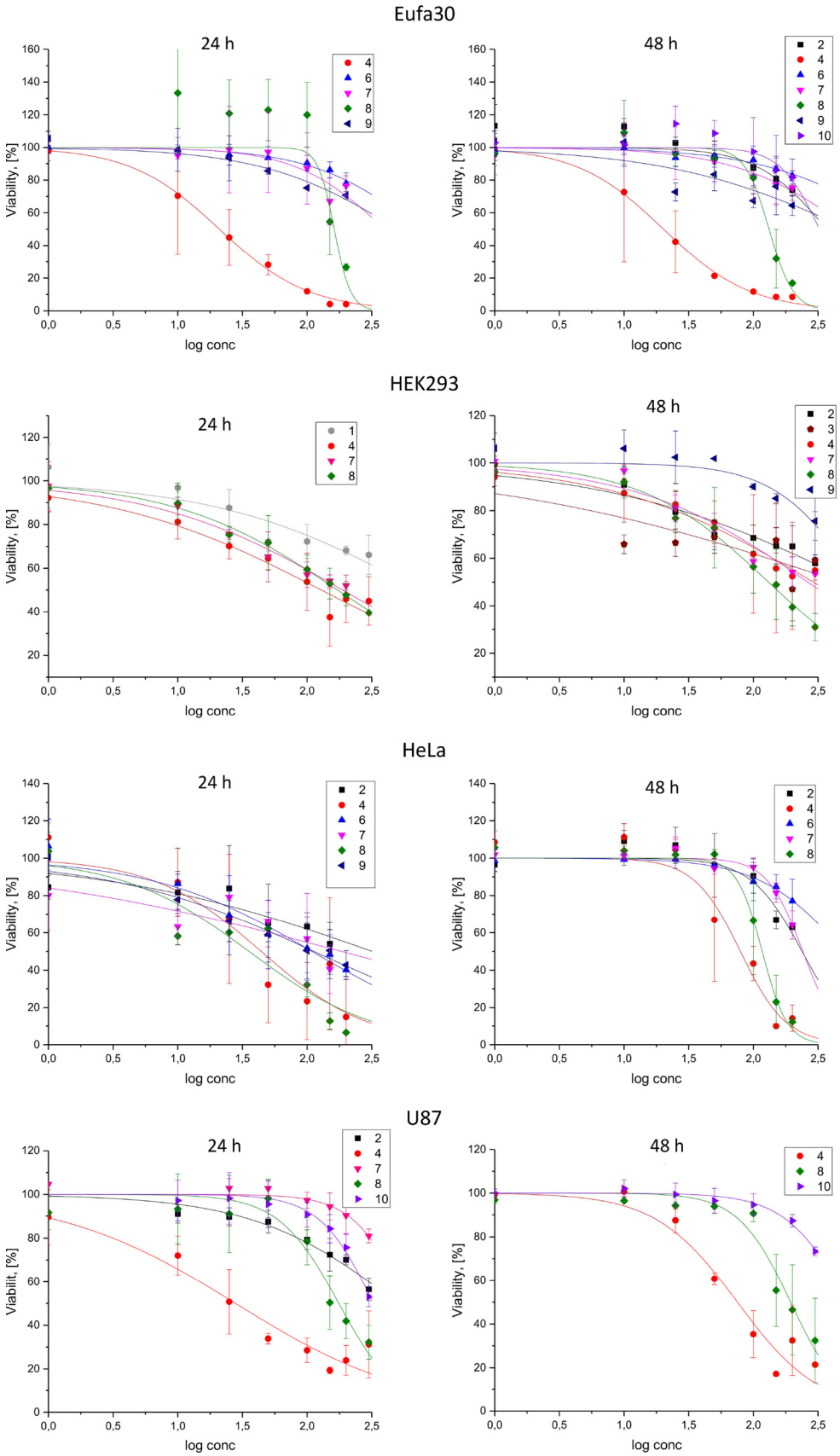

Fig. 4. The cytotoxic effect of indicated stilbene and dibenzo[*b,f*]oxepin derivatives on normal EUFA30 and HEK293 cells and cancerous HeLa and U87 cells based on AlamarBlue assay after 24 and 48 h of treatment. Non-linear fitting with a logistic dose-response model was employed and IC_{50} values calculated if possible (see Table 1).

Table 1
IC_{50} (μM) of tested dibenzo[*b,f*]oxepine (**1**,**3**,**4**) and stilbene derivatives (**5-10**) based on the survival of EUFA30, HEK293, HeLa, and U87 cells after 24 and 48 h of treatment. "*" - The predicted IC_{50} (above the maximum concentration tested – 300 μM), "N/A" –the IC_{50} could not be calculated.

Compound		Eufa30		HEK293		HeLa		U87	
		24	48	24	48	24	48	24	48
oxepines	(**1**)	N/A	N/A	733.8*	N/A	N/A	N/A	N/A	N/A
	(**2**)	N/A	368.1*	N/A	592.6*	319.6*	238.0	506.7*	N/A
	(**3**)	N/A	N/A	N/A	346.4*	N/A	N/A	N/A	N/A
	(**4**)	21.0	20.2	129.1	290.8	44.2	79.4	28.0	75.3
stilbenes	(**5**)	N/A	N/A	N/A	N/A	N/A	N/A	N/A	N/A
	(**6**)	756.4*	819.3*	N/A	N/A	109.2	503.1*	N/A	N/A
	(**7**)	398.0*	562.3*	268.7	267.8	184.7	241.2	583.1*	N/A
	(**8**)	162.2	132.2	172.2	130.9	35.6	117.1	175.9	194.0
	(**9**)	504.4*	553.6*	N/A	644.0*	112.9	N/A	N/A	N/A
	(**10**)	N/A	324.4*	N/A	N/A	298.8	N/A	168.5	600.4*

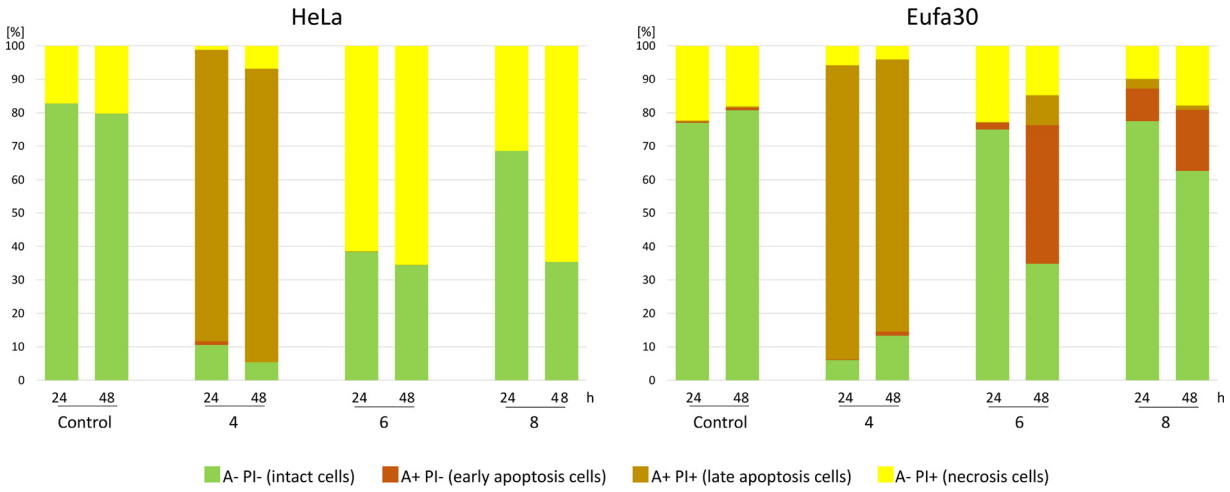

Fig. 5. Flow cytometry analysis of Eufa30 and HeLa cells stained with Annexin-FITC (A) and propidium iodide (PI) of (**4**), (**6**) and (**8**).

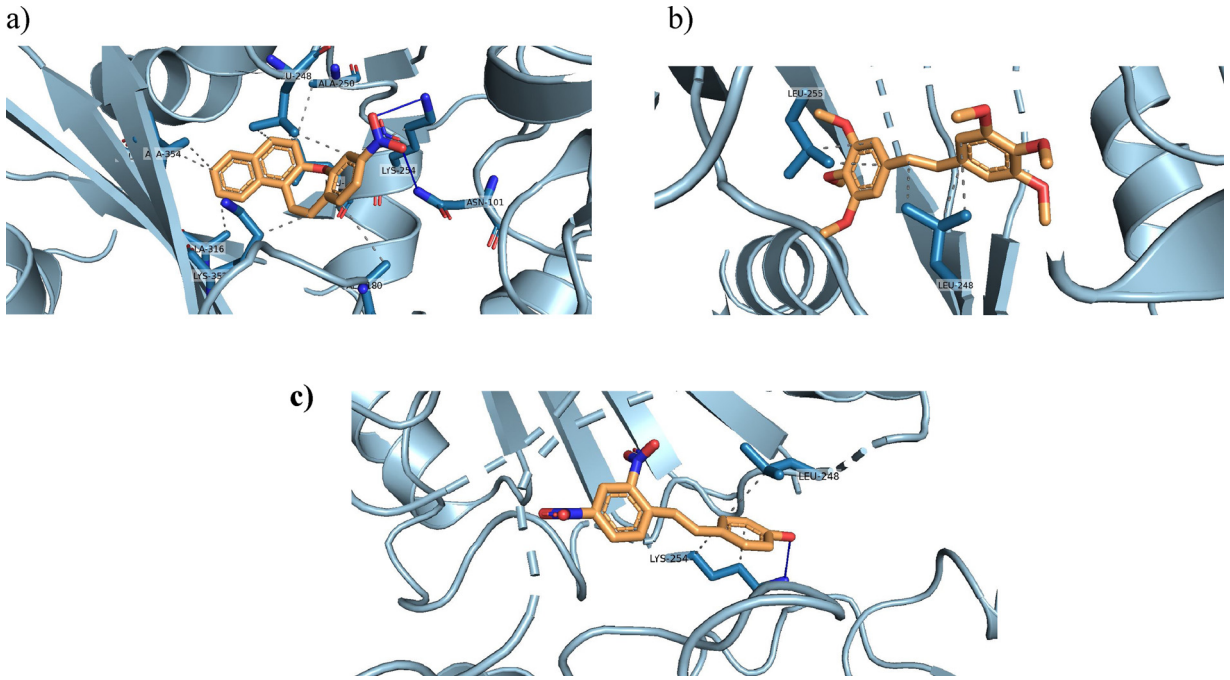

Fig. 6. 3D model of the interaction between compounds: a) (**4**), b) (**6**) c) (**8**) and the colchicine binding site of α and β tubulin (crystal structure from PDB code: 1SA0).

Declaration of Competing Interest

None.

Acknowledgment

This work was supported by the Faculty of Chemistry at Warsaw University of Technology.

Appendix A. Supplementary data

Supplementary material related to this article can be found, in the online version, at doi:https://doi.org/10.1016/j.biopha.2019.109781.

References

[1] M.A. Jordan, L. Wilson, Microtubules as a target for anticancer drugs, Nat. Rev. Cancer 4 (2004) 253-25.
[2] X. Dai, C. Tan, Combination of microRNA therapeutics with small-molecule anticancer drugs: mechanism of action and co-delivery nanocarriers, Adv. Drug. Deliv. Rev. 81 (2015) 184-17.
[3] N.M. Rusan, C.J. Fagerstrom, A.M. Yvon, P. Wadsworth, Cell cycle-dependent changes in microtubule dynamics in living cells expressing green fluorescent protein-alpha tubulin, Mol. Biol. Cell 12 (2001) 971–980.
[4] C. Dumontet, M.A. Jordan, Microtubule-binding agents: a dynamic field of cancer therapeutics, Nat. Rev. Drug Discov. 9 (2010) 790–803.
[5] R. Altaha, T. Fojo, E. Reed, J. Abraham, Epothilones: A Novel Class of Non-taxane Microtubule-stabilizing Agents, Curr. Pharm. Des. 8 (2002) 1707–1712.
[6] R.A. Stanton, K.M. Gernert, J.H. Nettles, R. Aneja, Drugs that target dynamic microtubules: a new molecular perspective, Med. Res. Rev. 31 (2011) 443–481.
[7] G. Wang, Z. Peng, J. Zhang, J. Qiu, Z. Xie, Z. Gong, Synthesis, biological evaluation and molecular docking studies of aminochalcone derivatives as potential anticancer agents by targeting tubulin colchicine binding site, Bioorg. Chem. 78 (2018) 332–340.
[8] W. Li, H. Sun, S. Xu, Z. Zhu, J. Xu, Tubulin inhibitors targeting the colchicine binding site: a perspective of privileged structures, Fut. Med. Chem. (2017), https://doi.org/10.4155/fmc-2017-0100.
[9] K. Donthiboina, P. Anchi, P.V. Sri Ramya, S. Karri, G. Srinivasulu, C. Godugu, N. Shankaraiah, A. Kamal, Synthesis of substituted biphenyl methylene indolinones as apoptosis inducers and tubulin polymerization inhibitors, Bioorg. Chem. 86 (2019) 210–223.
[10] A. Kamal, P.S. Srikanth, M.V.P.S. Vishnuvardhan, G. Bharath Kumar, K.S. Babu, S.M.A. Hussaini, J.S. Kapure, A. Alarifi, Combretastatin linked 1,3,4-oxadiazole conjugates as a Potent Tubulin Polymerization inhibitors, Bioorg. Chem. 65 (2016) 126–136.
[11] S.N.A. Bukhari, G.B. Kumar, H.M. Revankar, H.-L. Qin, Development of combretastatins as potent tubulin polymerizationinhibitors, Bioorg. Chem. 72 (2017) 130–147.
[12] J. Zhou, P. Giannakakou, Targeting microtubules for cancer chemotherapy, Curr. Med. Chem. Anti-Cancer Agents 5 (2005) 65–71.
[13] G.C. Tron, T. Pirali, G. Sorba, F. Pagliai, S. Busacca, A.A. Genazzani, Medicinal chemistry of combretastatin A4: present and future directions, J. Med. Chem. 11 (2006) 3033–3044.
[14] P. Hinnen, F.A.L.M. Eskens, Vascular disrupting agents in clinical development, Br. J. Cancer 8 (2007) 1159–1165.
[15] H. Lin, S. Chiou, C.W. Wu, W.B. Lin, L.H. Chen, Y.P. Yang, M.L. Tsai, Y.H. Uen, J.P. Liou, C.W. Chi, Combretastatin A4-induced differential cytotoxicity and reduced metastatic ability by inhibition of AKT function in human gastric cancer cells, J. Pharmacol. Exp. Ther. 323 (2007) 365–373.
[16] T. Fifis, L. Nguyen, C.L. Malcontenti-Wilson, S. Chan, P.L. Nunes Costa, J. Daruwalla, M. Nikfarjam, V. Muralidharan, M. Waltham, E.W. Thompson, C. Christophi, Treatment with the vascular disruptive agent OXi4503 induces an immediate and widespread epithelial to mesenchymal transition in the surviving tumor, Cancer Med. 2 (2013) 595–610.
[17] J. Cummings, M. Zweifel, N. Smith, P. Ross, J. Peters, G. Rustin, C. Dive, Evaluation of cell death mechanisms induced by the vascular disrupting agent OXi4503 during a phase I clinical trial, Br. J. Cancer 11 (2012) 1766–1771.
[18] D.W. Siemann, W. Shi, Dual targeting of tumor vasculature: combining avastin and vascular disrupting agents (CA4P or OXi4503), Anticancer Res. 28 (4B) (2008) 2027–2031.
[19] Information about fosbretabulin on https://clinicaltrialsgov/ct2/home.
[20] G. Likhtenshtein, Stilbenes. Applications in Chemistry, Life Sciences and Materials Science, WILEY-VCH Verlag GmbH & Co. KGaA, 2010.
[21] J.H. Goldie, A.J. Coldman, Drug Resistance in Cancer: Mechanisms and Models, Cambridge University Press, 2009.
[22] S.J. Lunt, S. Akerman, S.A. Hill, M. Fisher, V.J. Wright, C.C. Reyes-Aldasoro, G.M. Tozer, Ch Kanthou, Vascular effects dominate solid tumor response to treatment with combretastatin A-4-phosphate, Int. J. Cancer 129 (2011) 1979–1989.
[23] A. Kanakkanthara, P.H. Teesdale-Spittle, J.H. Miller, Cytoskeletal alterations that confer resistance to anti-tubulin chemotherapeutics, Anti-Cancer Agents Med. Chem. 13 (2013) 147–158.
[24] C. Stengel, S.P. Newman, M.P. Leese, B.V. Potter, M.J. Reed, A. Purohit, Class III β-tubulin expression and in vitro resistance to microtubule targeting agents, Br. J. Cancer 102 (2010) 316–324.
[25] J. Jakubowska, J. Mikuła-Pietrasik, K. Książek, H. Krawczyk, Cytotoxicity studies of novel combretastatin and pterostilbene derivatives, Biomed Res. Int. 8 (2014), https://doi.org/10.1155/2014/320895 Article ID 320895.
[26] H. Krawczyk, M. Wrzesiński, D. Mielecki, P. Szczeciński, E. Grzesiuk, Synthesis of derivatives of methoxydibenzo[*b, f*]oxepine in the presence of sodium azide, Tetrahedron 72 (2016) 3877–3884.
[27] P. Tobiasz, M. Poterała, E. Jaśkowska, H. Krawczyk, Synthesis and investigation of new cyclic molecules using the stilbene scaffold, RSC Adv. 8 (2018) 30678–30682.
[28] E. Tojo, D. Dominguez, L. Castedo, Alkaloids from Sarcocapnos enneaphylla, Phytochemistry 30 (1991) 1005–1010.
[29] T.-X. Qian, L.-N. Li, Isosalvianolic acid C, a depside possessing a dibenzooxepin skeleton, Phytochemistry 31 (1992) 1068–1070.
[30] Y.H. Lu, C.N. Lin, H.H. Ko, S.Z. Yang, L.T. Tsao, J.P. Wang, Novel anti-inflammatory constituents of Artocarpus rigida, Helv. Chim. Acta 86 (2003) 2566–2572.
[31] G.R. Pettit, A. Numata, C. Iwamoto, Y. Usami, T. Yamada, H. Ohishi, G.M.J. Cragg, Antineoplastic agents. 551. Isolation and structures of bauhiniastatins 1-4 from Bauhinia purpurea, J. Nat. Prod. 69 (2006) 323–327.
[32] P. Kittakoop, S. Nopichai, N. Thongon, P. Charoenchai, Y. Thebtaranonth, Bauhinoxepins a and B: new antimycobacterial dibenzo[b,f]oxepins from Bauhinia saccocalyx, Helv. Chim. Acta 87 (2004) 175–179.
[33] G. Han, J. Xia, J. Gao, Y. Inagaki, W. Tang, N. Kokudo, *Anti*-tumor effects and cellular mechanisms of resveratrol, Drug Discov. Ther. 9 (2015) 1–12.
[34] M. Tolomeo, S. Grimaudo, A. Di Cristina, M. Roberti, et al., Pterostilbene and 3'-hydroxypterostilbene are effective apoptosis-inducing agents in MDR and BCR-ABL-expressing leukemia cells, Int. J. Biochem. Cell Biol. 37 (2005) 1709–1726.
[35] P. Ferrer, M. Asensi, R. Segarra, A. Ortega, M. Benlloch, E. Obrador, M.T. Varea, G. Asensio, L. Jordá, J.M. Estrela, Association between pterostilbene and quercetin inhibits metastatic activity of B16 melanoma, Neoplasia 7 (2005) 37–47.
[36] C.M. Remsberg, J.A. Yanez, Y. Ohgami, K.R. Vega-Villa, A.M. Rimando, N.M. Davies, Pharmacometrics of pterostilbene: preclinical pharmacokinetics and metabolism, anticancer, antiinflammatory, antioxidant and analgesic activity, Phytother. Res. 22 (2008) 169–179.
[37] N. Suh, S. Paul, X. Hao, B. Simi, H. Xiao, A.M. Rimando, B.S. Reddy, Pterostilbene, an active constituent of blueberries, suppresses aberrant crypt foci formation in the azoxymethane-induced colon carcinogenesis model in rats, Clin. Cancer Res. 13 (2007) 350–355.
[38] D. Garbicz, D. Mielecki, M. Wrzesiński, T. Pilżys, M. Marcinkowski, J. Piwowarski, J. Dębski, E. Palak, P. Szczeciński, H. Krawczyk, E. Grzesiuk, Evaluation of *anti*-cancer activity of stilbene and methoxydibenzo[*b,f*]oxepin derivatives, Curr. Cancer Drug. Tar. 18 (2018) 706–717.
[39] X. Weng, L. Ren, L. Weng, J. Huang, S. Zhu, X. Zhou, L. Weng, Synthesis and Biological Studies of Inducible DNA Cross-Linking Agents, Angew. Chem. Int. Ed. 46 (2007) 8020–8023.
[40] J. Tomasi, B. Mennucci, R. Cammi, Quantum mechanical continuum solvation models, Chem. Rev. 105 (2005) 2999–3093.
[41] M.J. Frisch, G.W. Trucks, H.B. Schlegel, G.E. Scuseria, M.A. Robb, J.R. Cheeseman, J.A. Montgomery, T. Vreven, K.N. Kudin, J.C. Burant, J.M. Millam, S.S. Iyengar, J. Tomasi, V. Barone, B. Mennucci, M. Cossi, G. Scalmani, N. Rega, G.A. Petersson, H. Nakatsuji, M. Hada, M. Ehara, K. Toyota, R. Fukuda, J. Hasegawa, M. Ishida, T. Nakajima, Y. Honda, O. Kitao, H. Nakai, M. Klene, X. Li, J.E. Knox, H.P. Hratchian, J.B. Cross, V. Bakken, C. Adamo, J. Jaramillo, R. Gomperts, R.E. Stratmann, O. Yazyev, A.J. Austin, R. Cammi, C. Pomelli, J.W. Ochterski, P.Y. Ayala, K. Morokuma, G.A. Voth, P. Salvador, J.J. Dannenberg, V.G. Zakrzewski, S. Dapprich, A.D. Daniels, M.C. Strain, O. Farkas, D.K. Malick, A.D. Rabuck, K. Raghavachari, J.B. Foresman, J.V. Ortiz, Q. Cui, A.G. Baboul, S. Clifford, J. Cioslowski, B.B. Stefanov, G. Liu, A. Liashenko, P. Piskorz, I. Komaromi, R.L. Martin, D.J. Fox, T. Keith, M.A. Al-Laham, C.Y. Peng, A. Nanayakkara, M. Challacombe, P.M.W. Gill, B. Johnson, W. Chen, M.W. Wong, C. Gonzalez, J.A. Pople, Gaussian 03, Revision E.01, Gaussian, Wallingford, CT, 2004.
[42] R.B. Ravelli, B. Gigant, P.A. Curmi, I. Jourdain, S. Lachkar, A. Sobel, M. Knossow, Insight into tubulin regulation from a complex with colchicine and a stathmin-like domain, Nature 428 (2004) 198–202.
[43] RCSB Protein Data Bank -RCSB PDB, http://www.rcsb.org/pdb/home/home.do.
[44] O. Trott, A.J. Olson, AutoDock Vina: improving the speed and accuracy of docking with a new scoring function, efficient optimization and multithreading, J. Comput. Chem. 31 (2010) 455–461 Pettersen E F, Goddard T D, Huang C C, Couch G S, Greenblatt D M, Meng E C, Ferrin T E, UCSF Chimera–a visualization system for exploratory research and analysis. J. Comput. Chem., 2004, 25:1605-1612 http://vina.scripps.edu).
[45] The PyMOL Molecular Graphics System, Version 1.3, Schrödinger LLC, 2010.
[46] S. Salentin, S. Schreiber, V.J. Haupt, M.F. Adasme, M. Schroeder, PLIP: fully automated protein-ligand interaction profiler, Nucleic Acids Res. 43 (2015) W443–W447.
[47] T. Hattori, R. Takakura, S. Ueda, Y. Sawama, Y. Monguchi, H. Sajiki, Heterogeneous one-pot carbonylation and Mizoroki–Heck reaction in a parallel manner following the cleavage of cinnamaldehyde derivatives, Chem. Eur. J. 23 (2017) 8196–8202.
[48] G.C. Tron, T. Pirali, G. Sorba, F. Pagliai, S. Busacca, A.A. Genazzani, Medicinal chemistry of combretastatin A4: present and future directions, J. Med. Chem. 49 (2006) 3033–3044 Luo Y, Qiu K M, Lu X, Liu K, Fu J, Zhu H L, Synthesis, biological evaluation, and molecular modeling of cinnamic acyl sulfonamide derivatives as novel antitubulin agents. Bioorg. Med. Chem., 2011, 19: 4730-4738.
[49] Q. Zhang, Y.Y. Peng, X.I. Wang, S.M. Keenan, S. Arora, W.J. Welsh, Highly potent triazole-based tubulin polymerization inhibitors, J. Med. Chem. 50 (2007) 749–754.
[50] A. Massarotti, A. Coluccia, R. Silvestri, G. Sorba, A. Brancale, The tubulin colchicine domain: a molecular modeling perspective, Chem. Med. Chem. 7 (2012) 33–42.